Islamic Azad University

Journal of

Optoelectronical Nanostructures

Spring 2018 / Vol. 3, No. 2

Substrate Effects on the Structural Properties of Thin Films of Lead Sulfide

Sohrab Manouchehri[*,1], Javad Zahmatkesh[1], Mohammad Hassan Yousefi[1]

[1]Department of Physics, Faculty of Science, Malek Ashtar University of Technology, Shahinshahr, Isfahan, Iran.

(Received 12 Mar. 2018; Revised 16 Apr 2018; Accepted 27 May 2018; Published 15 Jun. 2018)

Abstract: Nanocrystalline PbS thin films are deposited on glass and alumina substrates through the chemical bath deposition technique by creating similar conditions, in order to investigate the effects of the substrate. The structural and optical properties of PbS films are investigated by X-ray diffraction, scanning electron microscope, and UV–Vis. The structural analyses of the films indicate that they are of polycrystalline configurations and have a face-centered-cubic (fcc) rock-salt structure on different substrates. The X-ray diffraction shows that the structure peaks occur at slightly higher angles in the deposited (grown) films on glass substrate than the ones deposited on alumina substrate. Crystal parameters are exceptionally affected by the type of substrate as well. SEM images reveal that the surface morphology of the PbS thin films is quite dependent upon the nature of the substrate. The optical band gaps of the samples are found to be 1.521 eV for glass and 1.678 eV for alumina substrates, which are higher in comparison to the bulk value (0.41 eV). According to the obtained results, PbS thin film on alumina substrate has narrower particle size distribution, better transmission and lower stress than PbS thin film on glass substrate.

Keywords: Chemical Bath Deposition, Optical Properties, Pbs Thin Film, Structural Properties, Substrate

1. INTRODUCTION

Lead sulphide (PbS) is an important direct narrow gap semiconductor material with tunable band gap depending on the size of quantum dots and a relatively large excitation Bohr radius of 18 nm [1, 2]. PbS nanoparticles are applied in light-emitting diodes, high-speed switching, solar cells, and IR detectors [2, 3].

PbS thin films are prepared by using various methods and techniques including successive ionic layer adsorption and reaction (SILAR), spray

* Corresponding author. E-mail: **dez283@yahoo.com**

pyrolysis, thermal evaporation, electro deposition (ED) as well as the chemical bath deposition (CBD) technique [4,5]. The CBD technique has been exploited for the deposition of thin chalcogenide films, because of such superior advantages as low cost, high-quality, and also producing homogeneous thin films. The CBD offers capability of deposing thin films on substrates of various kinds, shapes, and sizes [5].

The substrate nature plays an important role in preparing the thin films of PbS. It has been demonstrated that the substrate can affect the structure and thickness of the deposited layers [6]. PbS thin films usually were deposited chemically on glass [5-8] and the effect of different solution temperatures, various deposition times, varying the film thickness on the band gap, structural and morphological properties of PbS thin films are investigated.

Also, there are some reports for deposition of PbS thin films on other substrates such as: Si, Ge, GaAs [6], polymide [9] and the effects of substrate types on the structural properties of the films were studied and it is found that a large lattice mismatch between the substrate and PbS results in formation of coarse-grained layers with a small effective thickness and close matching of lattice constants leads to deposition of thicker layers with smaller grain size. However, there are few reports on the effect of substrates on optical constants. Some of them were discussed in the result and discussion section.

On the other hand, there is no report on depositing PbS on the alumina substrate. Glass and semiconductor substrates are used for deposition of PbS thin films and other substrates have not been investigated. Alumina has a good mechanical and thermal resistant which make it a good candidate for growth PbS thin film. Also, the alumina crystalline planes distances are close to crystalline planes distances of lead sulfide, which can reduce stress.

The present research aims at depositing thin films of PbS on glass and also for the first time on the alumina substrate, and afterwards, it investigates the effect of the substrate on crystallization, morphology, and optical properties of the PbS thin films.

2. EXPERIMENTAL METHODS AND MATERIALS

By employing the CBD technique, PbS thin films were deposited on glass and alumina substrates. A mixture of aqueous solutions of lead nitrate, sodium hydroxide, and thiourea was used in 2:1:2 molar ratios. All the raw materials having the purity levels higher than 99% were procured from Merck Co.

Cleaning the substrate surface is crucially important in order to obtain premium quality thin films. Thus, the substrates were cleaned in an ultrasonic cleaner with acetone, ethanol, and tripled distilled water. The cleaned substrates were vertically immersed in a beaker containing the mixture solution. The

deposition of PbS thin films were implemented at constant room temperature for 90 minutes. The samples deposited on glass and alumina substrates were designated at PbS1 and PbS2, respectively. After the deposition process, the films were cleaned using triply distilled water and then dried by placing the samples at room temperature.

The X-ray diffraction patterns of the samples were recorded on a PAN analytical X'Pert Pro MPD X-ray diffraction with Cu-Kα radiation (λ=1.5406 Å). The lattice parameter of PbS thin films can be determined by the following relations:

$$2d\ sin\theta = m\lambda \quad (1)$$

$$d = a/\sqrt{h^2 + k^2 + l^2} \quad (2)$$

Where d is the interplanar spacing, θ is the diffraction angle, m is an integer, h, k, and l are the Miller indices and a is the lattice parameter.

The degree of the crystallinity of the PbS thin films is quantitatively evaluated. Invoking this method, 'sum of net area'/'sum of total area' in PAN analytical X'Pert High Score software is the criterion for the degrees of crystallinity [10].

The surface morphology of the PbS thin films are examined by a scanning electron microscope (Tescan, VEGA II). UV–Vis spectrophotometer (P70 UV-Vis spectrometer PG Instrument Npd) is used to record the UV–Vis absorption and transmission of the samples in the range of 300-950 nm. To this end, the substrates are utilized as baseline and only the absorption and transmission of the thin films are recorded.

3. RESULTS AND DISCUSSION

A. Structural properties

The thicknesses of the PbS thin films measured by an optical interferometer are found to be about 250 nm and 350 nm, for the samples PbS1 and PbS2, respectively. The thickness of PbS thin films varies under equal conditions depending on the nature of the substrate.

Fig. 1 shows the XRD patterns of alumina substrate and the nanocrystalline PbS thin films. The diffraction peaks reveal the face-centered-cubic (fcc) rock-salt structure of PbS confirmed by the standard X-ray diffraction data files with the Reference No.77-0244.

PbS1 is deposited on the glass substrate and glass is an amorphous material. Therefore for sample PbS1, glass has not any peaks in X-ray diffraction pattern of PbS1 and we can only observe the peaks of PbS1.

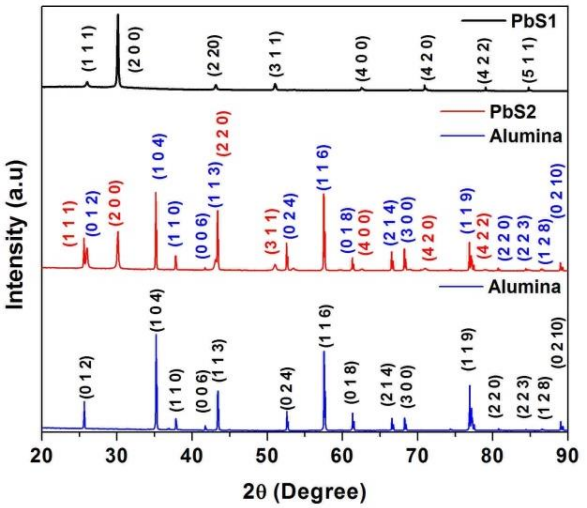

Fig. 1. XRD patterns of alumina substrate and nanocrystalline PbS thin films

The thickness of PbS2 thin film is about 350 nm and X-ray can penetrate through the sample up to 10 micrometers, so X-ray will pass through the sample and receive to the substrate. Consequently, in addition to PbS2 peaks, the peaks of alumina substrate will appear in the diffraction pattern.

According to the relative intensity given in Fig. 1, there is a preferred growth along the (200) plane for PbS1 and the (220) plane in the case of PbS2. One might conclude that the preferential growth and the crystallite sizes are dependent upon the employed substrates.

In comparison to the bulk sample, the position of peaks in the two samples is shifted to higher angles, which is higher in the case of PbS1 than PbS2. The shifts in the position of the peaks for PbS1 and PbS2 can be ascribed to stress. Stress changes the position of peaks, leading to the change in the lattice parameter.

The average stress (S) and micro strain (ε) are calculated using the following relations:

$$S = \{\frac{(a_0 - a)}{a_0}\}\frac{Y}{2\sigma} \quad (3)$$

$$\varepsilon = \frac{(a_0 - a)}{a_0} \quad (4)$$

Where a and a_0 are the corrected values for the lattice parameter of the thin film sample and the lattice parameter of the bulk sample, Y and σ are the Young's modulus and Poisson's ratio of the bulk sample, respectively. For PbS, Y is equal to 70.2 GPa and σ is 0.28 [11].

The corrected value of 'a' is estimated from Nelson-Riley plots by plotting

'a' against the error function:

$$f(\theta) = \frac{1}{2}\left(\frac{cos^2\theta}{sin\theta} + \frac{cos^2\theta}{\theta}\right) \quad (5)$$

and by extrapolating the plot to $\theta = 90^{\circ}$ [12]. The Nelsone-Riley plots for PbS thin films are shown in Fig. 2.

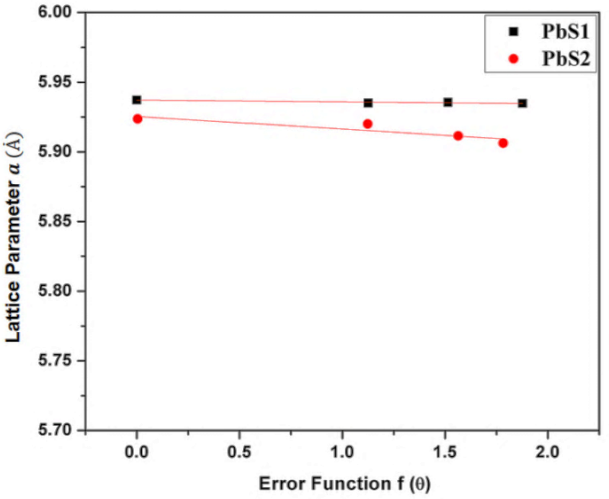

Fig. 2. Lattice parameter as a function of the error function. Nelsone-Riley plots for samples of PbS thin film

The total stress in the thin films is due to (i) differences between the thermal expansion coefficient of the thin films and substrates, (ii) the lattice mismatch between the thin films and the substrates as well as the other crystallographic faults that might exist in the thin films. If there is a simultaneous broadening of size and strain, the strain and crystallite size can be obtained according to the Williamson–Hall (W-H) plot using the following equation [13]:

$$\frac{\beta cos\theta}{\lambda} = \frac{1}{D} + \frac{4\varepsilon sin\theta}{\lambda} \quad (6)$$

Where β is the full width at half maximum of the diffraction peaks, D is the average crystallite size, and the other parameters are designated as those mentioned earlier. Fig. 3 displays the Williamson–Hall plots for the samples of the PbS thin film. The average strain in the film can be obtained from the slope of the plot, whereas the average crystallite size is the intercept of the plot on $\beta cos\theta$ axis. The structural parameters of the PbS thin films deposited at room temperature are listed in Table I. The deviation of the calculated lattice parameter 'a' from the strain free bulk sample (a_0 =5.936 Å) indicates that the films are subjected to strain.

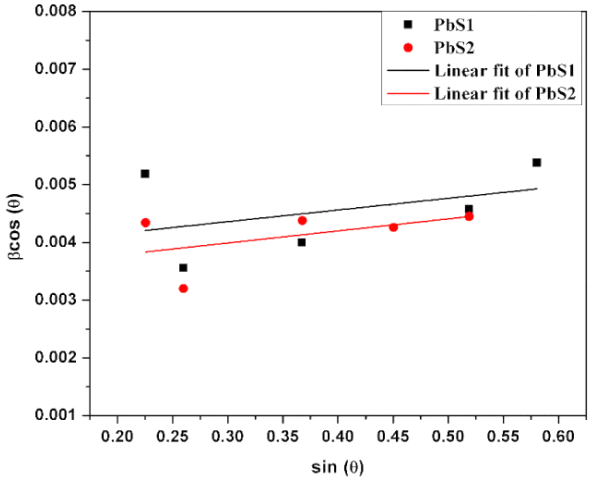

Fig. 3. Williamson–Hall plots for samples of PbS thin film for different substrates

TABLE I: STRUCTURAL PARAMETERS OF PBS THIN FILMS DEPOSITED AT ROOM TEMPERATURE

Sample	2θ (DEGREES)	d (Å)	a calculated (Å)	a corrected (Å)	$S \times 10^8 (\frac{N}{m^2})$	$\varepsilon \times 10^{-4}$
PbS1	26.055	3.411	5.906	5.922	3.378	2.695
	30.113	2.959	5.920			
	43.135	2.092	5.911			
	53.531	1.710	5.923			
	62.522	1.485	5.940			
PbS2	26.005	3.426	5.934	5.935	1.266	1.010
	30.115	2.967	5.935			
	43.107	2.098	5.935			
	53.414	1.713	5.937			
	62.531	1.484	5.936			

From W–H plots of the films (Fig. 3), it can be confirmed that the X-ray line broadening in polycrystalline PbS thin films is brought about by the effects of size and the strain. The lattice constant 'a' is found to be different by changing the substrates and in the case of PbS2, it is greater than that of PbS1 and closer to the bulk one. The change in the lattice constant for the deposited thin film over the bulk clearly suggests that the film grains are strained. The average crystallite sizes are found by Williamson–Hall plot. The crystallinity and average crystallite sizes are listed in Table II.

TABLE II: COMPARISON OF '*D*' VALUES FOR PBS THIN FILMS DEPOSITED AT ROOM TEMPERATURE

Sample	Average crystallite size [*D* (nm)]	Crystallinity (%)
PbS1	48	45
PbS2	47	53

The PbS thin film on the alumina substrate shows better crystallinity as compared with that of the glass substrate. This might be due to the crystalline structure of alumina substrate compared with that of amorphous glass, so less lattice imperfection would appear during the film growth process. Fig. 4 exhibits the relation between the crystallite size, the microstrain, and the substrates.

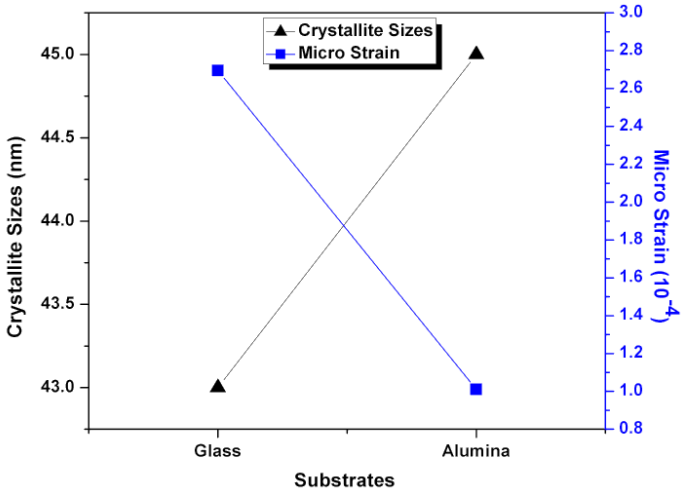

Fig. 4. Relation between crystallite size, microstrain, and substrates

It can be observed that by increasing the crystallinity, there will be an increase in the crystalline size while there will be a decrease in the microstrain of the PbS thin film. In addition, it is observed that the thickness of the films, which depends upon nature of the substrate, can affect the crystallinity which can be improved by increasing the PbS film thickness. In comparison, PbS1 has a higher shift in the position of X-ray peaks and a lower crystallinity due to the higher stress.

B. Morphology

The surface morphology of the films is affected by a variety of factors including surface roughness of the substrate, adhesion strength of the film to the

substrate, differences in thermal expansion coefficients between the substrate and the film, and the thickness of the film.

Fig. 5 shows the surface of the deposited PbS thin films on glass and alumina substrates. The Sample ‘PbS2’ has an amazingly beautiful morphology. In fact, no report has been given to date of such a morphology for PbS thin films. We presume for PbS2 that the film formation begins via nucleation of islands, which then grows to cover the surface of the substrate and eventually accumulating to form a continuous film. Then, it is realized that the nature of the substrate substantially affects the growth of the PbS crystallites.

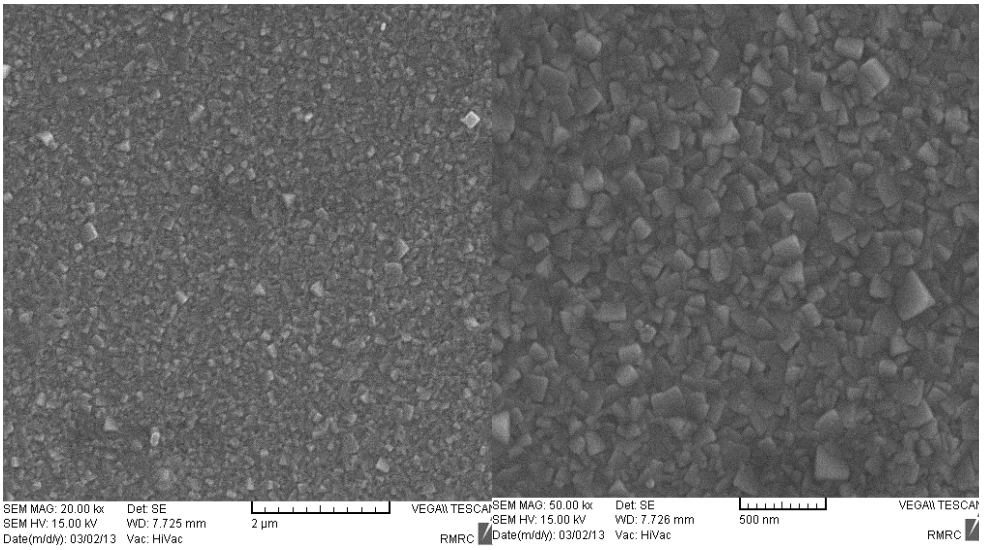

(a) (b)

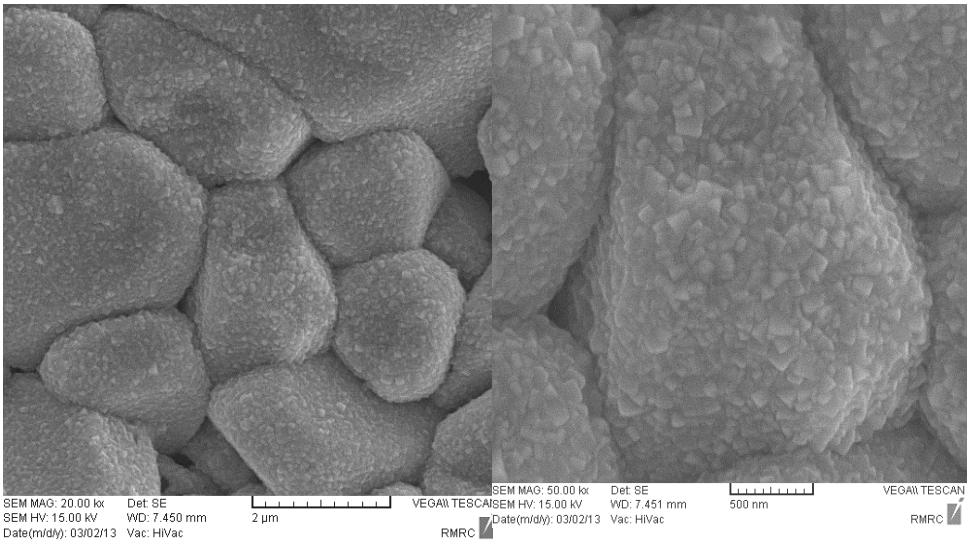

(c) (d)

Fig. 5. SEM images of nanocrystalline (a) and (b) PbS1, (c) and (d) PbS2 thin films with different magnification

It can be inferred from the appearances that both of our samples having dark surfaces have proper adherence to the substrate, whereas PbS1 has a uniform, smoothness, and mirror-like surface. The PbS2 surface is not mirror-like and has a lower reflection. Continuous and uniform films obtained on glass indicate good wetting of the substrate by PbS1.

The grain size distribution of the PbS thin films prepared on different substrates is shown by a histogram in the corresponding SEM results, as is shown in Fig. 6. More than 100 grains are investigated to obtain the average grain size. The estimated average grain sizes from SEM are about 100 nm for PbS1 and 110 nm for PbS2. Each grain is an aggregation of smaller nanocrystallites.

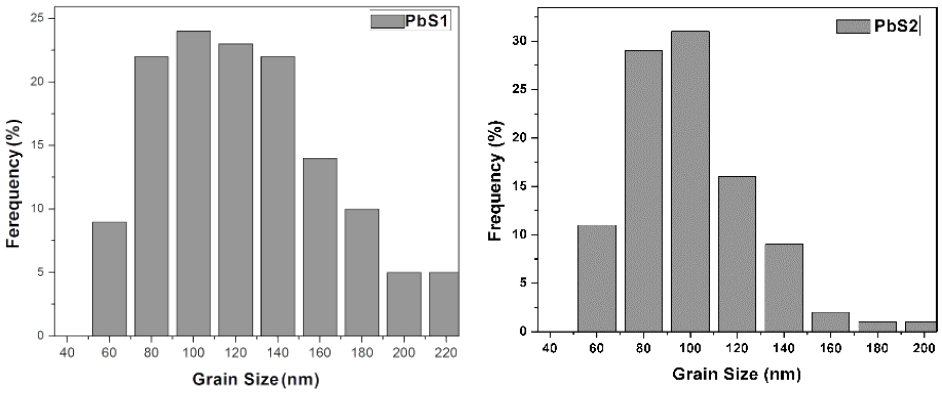

(a) (b)

Fig. 6. Grain size distribution of (a) PbS1 and (b) PbS2 thin films

C. Optical properties

A well-known fact is that exploring such optical properties as absorption and transmission is essential for applications in the optoelectronic devices. The UV–Vis absorption and transmission spectra of PbS thin films are displayed in Fig. 7.

The electronic transition between the valence and the conduction bands starts at the absorption edge corresponding to the minimum energy difference between the highest energy of the valence band and the lowest energy of the conduction band in the crystalline materials [14].

The clear absorption edges shown by all samples indicate the crystalline nature of the film (Fig. 7(a)). The absorption edge shifts towards the higher wavelength region for PbS2 as compared with PbS1. It is observed that the behavior of the absorption plots is not identical; a fact, which is due to differences in the substrates. The alumina substrate affects the morphology and structure of PbS2, which leads to a relative decrease in the absorption spectra.

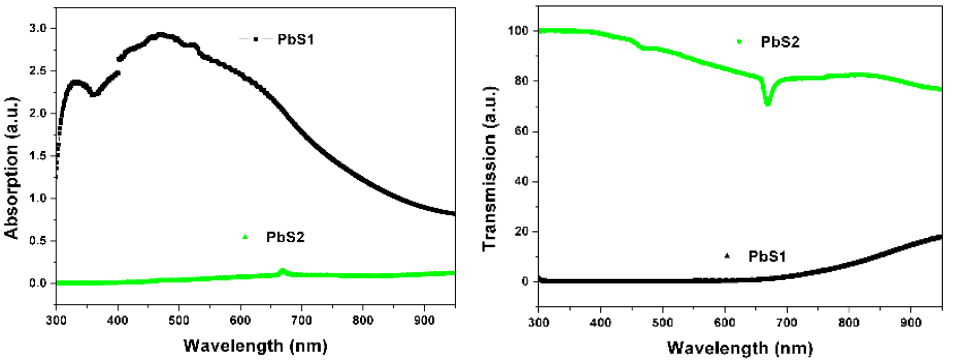

(a) (b)

Fig. 7. (a) UV–Vis absorption and (b) transmission spectra of PbS thin films as a function of wavelength

According to Fig. 7(b), the transmission increases with an increase in wavelength in the case of PbS1, but for PbS2, it decreases with an increase in the wavelength, while it slightly increases after that. It can be seen from Fig. 7(a) and (b), that the absorption and transmission of each sample are compatible.

The absorption and transmission spectra of PbS films are studied in order to evaluate the band gap (E_g), the refractive index (n), the extinction coefficient (k), and the dielectric constants ($\varepsilon_1$and ε_2).

The optical band gap E_g of the prepared thin films is calculated by means of the Tauc's relation:

$$\alpha h\nu = A(h\nu - E_g)^{\frac{1}{2}} \quad (7)$$

Where α is the absorption coefficient, ν is the incident photon frequency, h is the Planck's constant, and A is a constant [15].

Fig. 8 shows $(\alpha h\nu)^2$ versus $(h\nu)$ for calculating the optical band gap. The optical band gap is determined by extrapolating of the linear part with maximum slope of the curves to intercept the '$h\nu$' axis. The optical band gap is about 1.521 eV and 1.678 eV for the samples PbS1 and PbS2, respectively. The optical band gap of PbS2 is higher than PbS1, which is due to a decrease in the particle size and that can be attributed to the effect of substrate nature on the optical and structural properties of the thin films.

Some parts are always absorbed, when light passes through a medium. This can be conveniently taken into account by defining a complex index of refraction, $\mathrm{n} = n + ik$. Here, the real part of the refractive index n indicates the phase speed, while the imaginary part k (extinction coefficient) indicates the amount of absorption [16]. The extinction coefficient (k) is related to the amplitude

decay of the electric field oscillations as the wave penetrates in the medium [17].

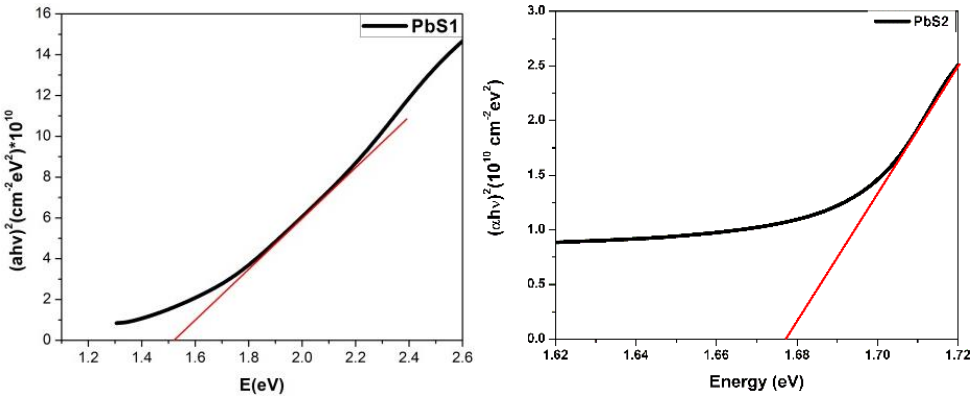

(a) (b)

Fig. 8. Variation of $(\alpha h\nu)^2$ versus energy ($h\nu$) for samples (a) PbS1 and (b) PbS2

The extinction coefficient 'k' can be calculated from the absorption coefficient using the following relation [17]:

$$k = \alpha\lambda / 4\pi \quad (8)$$

Fig. 9 shows the extinction coefficient variation with the wavelength. According to Fig. 9, the extinction coefficient of PbS1 is higher than that of PbS2, because it has more absorption than of PbS2. For PbS1, the extinction coefficient increases by an increase in the wavelength in the range of 300-600 nm, which is due to absorbance increment in the latter wavelength region. Also a decrease in

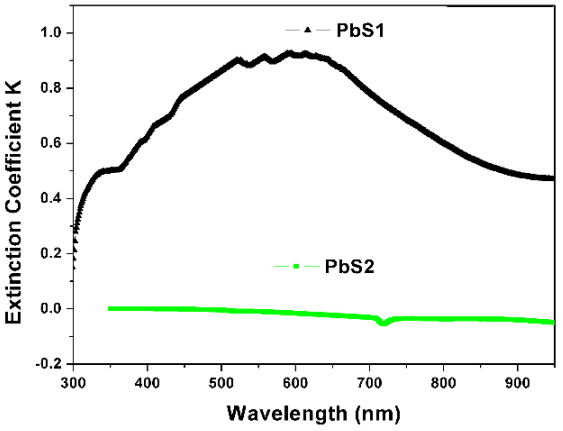

Fig. 9. Variations in extinction coefficients along with wavelengths

the PbS1 extinction coefficient in the wavelength range 600-950 nm and also in PbS2 in the whole range of wavelengths show that the absorbance decreases in these wavelength regions [18].

The real part of the refractive index (n) can be calculated using the following equation [19]:

$$n = \frac{1+R}{1-R} + [\frac{4R}{(1-R)^2} - k^2]^{\frac{1}{2}} \quad (9)$$

Where R is the reflected power. Fig. 10 shows the real part of the refractive index for all samples. A different behavior is shown by n variation of the films. The refractive index for PbS1 tends to decrease by an increase in the wavelength; whereas for PbS2, the plot of the refractive index is composed of two regions, i.e. the so-called abnormal and also the normal dispersions. The values of n of the PbS2 thin film increase with an increase in the abnormal dispersion region, while the refractive index values of the PbS2 thin film decrease with an increase in the wavelength of the normal dispersion region [20]. Values for the refractive index, PbS1, and PbS2, are not constant over the entire wavelength, and thus it implies the wavelength dependence [21].

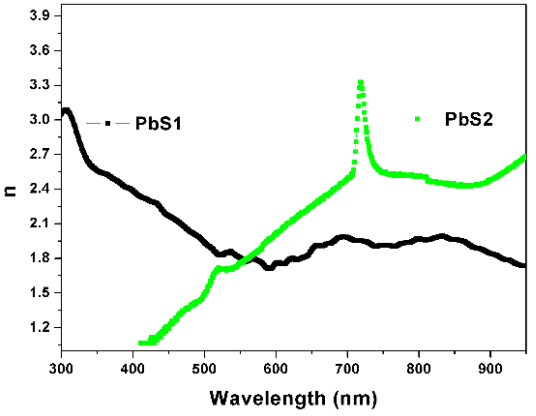

Fig. 10. Real part of refractive index for samples as function of wavelength

According to the results, the refractive index of PbS thin films can be optimized by changing the substrates. The complex dielectric constant is an intrinsic feature of the material. The real part of the dielectric constant indicates the ability of the material in storing the electromagnetic energy (or electric field energy), while the imaginary part indicates the ability of energy absorption from an electric field [22].

The real and the imaginary parts of the dielectric constant are calculated via following relations [23]:

$$\varepsilon_1 = n^2 - k^2 \quad (10\text{ a})$$

$$\varepsilon_2 = 2nk \quad (10\text{ b})$$

The real and imaginary part of the complex dielectric constant for PbS thin films are presented in Fig. 11(a) and (b).

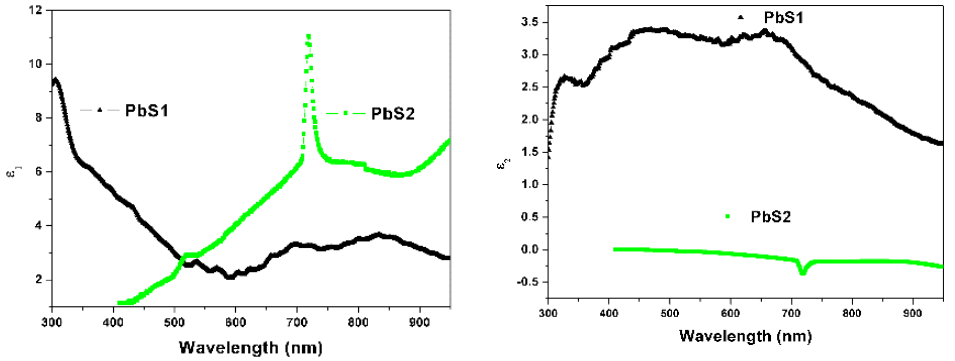

(a) (b)

Fig. 11. (a) Real and (b) imaginary part of complex dielectric constant for PbS thin films

The real part of the complex dielectric for PbS1 decreases by an increase in the wavelength, whereas in the case of PbS2, the real part of the dielectric constant increases with an increase in the wavelength until it reaches a high value, after which, it decreases as wavelength increases. The high value of the real part of dielectric constant indicates that the PbS films have the polarization ability.

The behavior of ε_1 is similar to that of the refractive index because of the smaller value of the k^2 in comparison with n^2, while the behavior of ε_2 is mainly dependent upon the values of k, the values of which are related to the variations in the absorption coefficient.

Table III shows thickness, band gap, and optical constant of our results and some references at the wavelength of 500 nm. As can be seen, their results are different and irregular. The thickness and band gap of our samples are close to the other reported result, but the optical constants are different. It is indicate that they can be dependent to the substrate nature and crystallinity.

TABLE III: COMPARISON OF THICKNESS, BAND GAP, AND OPTICAL CONSTANTS

Reference	Substrate	Thickness (nm)	Band gap (eV)	n	k	ε_1	ε_2
PbS1	glass	250	1.521	1.93	0.86	3.0	3.34
PbS2	alumina	350	1.678	1.49	0.01	2.2	0.01
[24]	Si	280	0.34	-	-	-	-
[25]	glass	110	2.5	5	0.6	22	4.35
[26]	glass	-	1.6	2	1.3	3.2	2
[27]	glass	386	1.6	2.2	0.01	3.8	0.04
[28]	glass	300	1.59	1	0.8	0.5	2.6

4. CONCLUSION

PbS nanocrystalline layers were chemically deposited on glass and alumina substrates. Under similar conditions, the thickness of the thin films varied depending upon the nature of the substrate. Such micro-structural parameters as lattice constant, crystallite size, internal stress, micro-strain, and optical properties of the synthesized PbS thin films were found to be affected by the chemical nature of the substrate.

SEM investigations indicated that the morphology of the layers is strongly influenced by the nature of the substrate. The examined optical properties show that the PbS thin film on alumina substrate is more transparent than the film deposited on glass substrate, which can be attributed to the effects on the morphological properties of the deposited substrate. Thus, by choosing the right substance, the optical and structural properties of PbS thin films can be enhanced to a considerable degree.

REFERENCES

[1] S. Seghaier, N. Kamoun, R. Brini, and A. Amara. *Structural and optical properties of PbS thin films deposited by chemical bath deposition.* Mater. Chem. Phys. [Online]. 97(1) (2006, May.) 71-80. Available: https://doi.org/10.1016/j.matchemphys.2005.07.061

[2] J. Tian, T. Shen, X. Liu, C. Fei, L. Lv, and G. Cao. *Enhanced performance of PbS-quantum-dot-sensitized solar cells via optimizing precursor solution and electrolytes.* Sci. rep. [Online]. 6 (2016, Mar.) 23094. Available: 10.1038/srep23094

D. Kumar, G. Agarwal, B. Tripathi, D. Vyas, and V. Kulshrestha. *Characterization of PbS nanoparticles synthesized by chemical bath deposition.* J. Alloys Compd. [Online]. 484(1) (2009, Sep.) 463-466. Available:

https://doi.org/10.1016/j.jallcom.2009.04.127

[3] S. Arabzade, M. Samadpour, and N. Taghavinia. *Sequential deposition as a route for efficient counter electrodes in quantum dot sensitized solar cells.* RSC Advances. [Online]. 5(57) (2015, May.) 45592-45598. Available: http://pubs.rsc.org/en/content/articlelanding/2015/ra/c5ra04401d#!divAbstract

[4] M. Abbas, A.A.M. Shehab, N. Hassan, and A. Al-Samuraee. *Effect of temperature and deposition time on the optical properties of chemically deposited nanostructure PbS thin films.* Thin Solid Films. [Online]. 519(15) (2011, May.) 4917-4922. Available: https://doi.org/10.1016/j.tsf.2011.01.053

[5] A.P. Gaiduk, P.I. Gaiduk, and A.N. Larsen. *Chemical bath deposition of PbS nanocrystals: Effect of substrate.* Thin Solid Films. [Online]. 516 (12) (2008, Apr.) 3791-3795. Available: https://doi.org/10.1016/j.tsf.2007.06.122

[6] A. Fouda, M. Marzook, H.A. El-Khalek, S. Ahmed, E. Eid, and A. El Basaty. *Structural and optical characterization of chemically deposited PbS thin films.* Silicon. [Online]. 9(6) (2017, Nov.) 809-816. Available: https://link.springer.com/article/10.1007/s12633-015-9399-z

[7] B. Abdallah, A. Ismail, H. Kashoua, and W. Zetoun. *Effects of deposition time on the morphology, structure, and optical properties of PbS thin films prepared by chemical bath deposition.* J. Nanomaterials. [Online]. 2018 (2018, May.) ID 1826959. Available: https://doi.org/10.1155/2018/1826959

[8] M. Faraj and M. Pakhuruddin. *Deposited lead sulfide thin films on different substrates with chemical spray pyrolysis technique*. Int. J. Thin. Fil. Sci. Tec. [Online]. 4(3) (2015) 215-217. Available: http://dx.doi.org/10.12785/ijtfst/040310

[9] S. Naghibi, M.A. Faghihi Sani, and H.R. Madaah Hosseini. *Application of the statistical Taguchi method to optimize TiO_2 nanoparticles synthesis by the hydrothermal assisted sol–gel technique.* Ceram. Int. [Online]. 40(3) (2014, Apr.) 4193-4201. Available: https://doi.org/10.1016/j.ceramint.2013.08.077

[10] M. Mozafari, F. Moztarzadeh, D. Vashaee, and L. Tayebi. *Effects of heat treatment on physical, microstructural and optical characteristics of PbS luminescent nanocrystals.* Physica E. [Online]. 44(7-8) (2012, Apr.–May.) 1429-1435. Available: https://doi.org/10.1016/j.physe.2012.03.006

[11] A. Hussain, A. Begum, and A. Rahman. *Characterization of nanocrystalline lead sulphide thin films prepared by chemical bath deposition technique.* Arab. J. Sci. Eng. [Online]. 38(1) (2013, Jan.) 169-174. Available: https://link.springer.com/article/10.1007%2Fs13369-012-0390-3

[12] N. Choudhury and B. Sarma. *Structural characterization of lead sulfide thin films by means of X-ray line profile analysis.* Bull. Mater. Sci. [Online]. 32(1) (2009, Feb.) 43-47. Available: https://link.springer.com/article/10.1007%2Fs12034-009-0007-y

[13] S. Kumar, T. Sharma, M. Zulfequar, and M. Husain. *Characterization of vacuum evaporated PbS thin films.* Physica B. [Online]. 325 (2003, Jan.) 8-16. Available: https://doi.org/10.1016/S0921-4526(02)01272-3

[14] K. Kamli, Z. Hadef, B. Chouial, B. Zaidi, B. Hadjoudja, and A. Chibani. *Synthesis and characterisation of tin sulphide thin films.* Surface Eng. [Online]. 33(8) (2017, Jan.) 567-572. Available: https://doi.org/10.1080/02670844.2016.1271593

[15] P. Barman and P. Sharma. *Optical studies of Se-Bi-Te-Sb thin films by single transmission spectrum.* Glass Phys. Chem. [Online]. 39(3) (2013, May.) 276-278. Available: https://link.springer.com/article/10.1134/S1087659613030048

[16] H. Kumar, P. Ram, and M. Singh. *Effect of rapid thermal annealing on optical properties of zinc sulphide thin films.* Surface Eng. [Online]. 33(3) (2017, Jul.) 181-185. Available: https://doi.org/10.1080/02670844.2016.1204130

[17] M. Mazilu, N. Tigau, and V. Musat. *Optical properties of undoped and Al-doped ZnO nanostructures grown from aqueous solution on glass substrate.* Opt. mater. [Online]. 34(11) (2012, Jun.) 1833-1838. Available: https://doi.org/10.1016/j.optmat.2012.05.010

[18] M.B. Rabeh and M. Kanzari. *Optical constants of Zn-doped $CuInS_2$ thin films.* Thin Solid Films. [Online]. 519(21) (2011, Jan.) 7288-7291. Available: https://doi.org/10.1016/j.tsf.2011.01.139

[19] F. El-Tantawyd, F. Yakuphanogluc, and W. Farooq. *Determination of Optical Constants of Nanocluster CdO Thin Films Deposited by Sol Gel Technique.* Acta Phys. Pol. A. [Online]. 126(3) (2014, Jul.) 798-807. Available: 10.12693/APhysPolA.126.798

[20] J. Akinlami and F. Bolaji. *Complex index of refraction of indium nitride InN. Semiconductor Physics.* Semicond. Phys. Quantum Electron. Optoelectron. [Online]. 15(3) (2012, Sep.) 276-280. Available: journal-spqeo.org.ua/n3_2012/v15n3-2012-p276-280.pdf

[21] E.D. Como, F.D. Angelis, H. Snaith, and A. Walker. *Unconventional Thin Film Photovoltaics.* The Royal Society of Chemistry, Cambridge, UK, 2016, 57-106. Available: http://dx.doi.org/10.1039/9781782624066

[22] H. Gao, J. Tian, H. Kong, P. Yang, W. Zhang, and J. Chu. *Optical and magnetic properties of mixed crystal $Ti_{0.95}Ni_{0.05}O_2$ films deposited on Si substrates by sol–gel method.* Surf. Coat. Technol. [Online]. 228 (2013, Aug.) 162-166. Available: https://doi.org/10.1016/j.surfcoat.2013.04.024

[23] A.S. Obaid, M.A. Mahdi, and Z. Hassan. *Growth of Nanocrystalline PbS Thin Films by Solid-Vapor Deposition.* Adv. Mater. Res. [Online]. 620(1) (2013, Jan.) 1-6. Available: https://doi.org/10.4028/www.scientific.net/AMR.620.1

[24] F. Göde, E. Güneri, F. Emen, V.E. Kafadar, and S. Ünlü. *Synthesis, structural, optical, electrical and thermoluminescence properties of chemically deposited PbS*

thin films. J. Lumin. [Online]. 147 (2014, Mar.) 41-48. Available: https://doi.org/10.1016/j.jlumin.2013.10.050

[25] C.O. Mosiori, W.N. Njoroge, and J. Okumu. *Optical and electrical properties of Pbs thin films grown by chemically bath deposition [CBD] at different lead concentrations*. Int. J. Adv. Res. Phys. Sci. [Online]. 1(1) (2014, May.) 25-32. Available: https://www.arcjournals.org/pdfs/ijarps/v1-i1/4.pdf

[26] I. Ikhioya, S. Ehika, and B. Ijabor. *Influence of Deposition Potential on Lead Sulphide (PbS) Thin Film Using Electrodeposition Technique*. Asian. J. Chem. Sci. [Online]. 3(4) (2018, Mar.) 1-8. Available: http://www.journalrepository.org/media/journals/AJOCS_55/2018/Mar/Lucky342018AJOCS40415.pdf

[27] S. Ahmad, S. Kasim, and L. Latif. *Effects of thermal annealing on structural and optical properties of nanocrystalline CdxPb1-xS thin films prepared by CBD*. Jordan. J. Phys. [Online]. 9(2) (2016, Oct.) 113-122. Available: http://journals.yu.edu.jo/jjp/JJPIssues/Vol9No2pdf2016/7.pdf